University of Plymouth

PEARL **https://pearl.plymouth.ac.uk**

01 University of Plymouth Research Outputs University of Plymouth Research Outputs

2007-12-01

Delta-like 4 Notch Ligand Regulates Tumor Angiogenesis, Improves Tumor Vascular Function, and Promotes Tumor Growth In vivo

Li, J-L

http://hdl.handle.net/10026.1/10302

10.1158/0008-5472.can-07-0969
Cancer Research
American Association for Cancer Research (AACR)

All content in PEARL is protected by copyright law. Author manuscripts are made available in accordance with publisher policies. Please cite only the published version using the details provided on the item record or document. In the absence of an open licence (e.g. Creative Commons), permissions for further reuse of content should be sought from the publisher or author.

Tumor and Stem Cell Biology

Cancer Research

DLL4-Notch Signaling Mediates Tumor Resistance to Anti-VEGF Therapy *In Vivo*

Ji-Liang Li[1], Richard C.A. Sainson[1], Chern Ein Oon[1], Helen Turley[1], Russell Leek[1], Helen Sheldon[1], Esther Bridges[1], Wen Shi[1], Cameron Snell[1], Emma T. Bowden[3], Herren Wu[3], Partha S. Chowdhury[3], Angela J. Russell[2], Craig P. Montgomery[2], Richard Poulsom[4], and Adrian L. Harris[1]

Abstract

Resistance to VEGF inhibitors is emerging as a major clinical problem. Notch signaling has been implicated in tumor angiogenesis. Therefore, to investigate mechanisms of resistance to angiogenesis inhibitors, we transduced human glioblastoma cells with retroviruses encoding Notch delta-like ligand 4 (DLL4), grew them as tumor xenografts and then treated the murine hosts with the VEGF-A inhibitor bevacizumab. We found that DLL4-mediated tumor resistance to bevacizumab *in vivo*. The large vessels induced by DLL4-Notch signaling increased tumor blood supply and were insensitive to bevacizumab. However, blockade of Notch signaling by dibenzazepine, a γ-secretase inhibitor, disrupted the large vessels and abolished the tumor resistance. Multiple molecular mechanisms of resistance were shown, including decreased levels of hypoxia-induced VEGF and increased levels of the VEGF receptor VEGFR1 in the tumor stroma, decreased levels of VEGFR2 in large blood vessels, and reduced levels of VEGFR3 overall. DLL4-expressing tumors were also resistant to a VEGFR targeting multikinase inhibitor. We also observed activation of other pathways of tumor resistance driven by DLL4-Notch signaling, including the FGF2-FGFR and EphB4-EprinB2 pathways, the inhibition of which reversed tumor resistance partially. Taken together, our findings show the importance of classifying mechanisms involved in angiogenesis in tumors, and how combination therapy to block DLL4-Notch signaling may enhance the efficacy of VEGF inhibitors, particularly in DLL4-upregulated tumors, and thus provide a rational base for the development of novel strategies to overcome antiangiogenic resistance in the clinic. *Cancer Res; 71(18); 6073–83. ©2011 AACR.*

Introduction

Tumor angiogenesis is essential for tumor growth and metastasis and is triggered by a variety of proangiogenic factors, regulated by many angiogenic pathways. The most important and best characterized is the VEGF pathway (1). Blockade of VEGF signaling inhibits tumor angiogenesis and growth in various preclinical models (2, 3) and having systemic effects (4). The effect of anti-VEGF strategy has been validated in randomized phase III clinical trials. Disruption of VEGF signaling by using bevacizumab, a humanized anti-human VEGF antibody or sorafenib and sunitinib, 2 small chemical inhibitors of receptor-tyrosine kinases (RTK) including VEGF receptors (5) have yielded a significant improvement in progression-free survival but rarely in overall survival for patients with several types of cancers including metastatic colorectal cancer (6), advanced non–small cell lung cancer (7), metastatic breast cancer (8), advanced clear-cell renal-cell carcinoma (9–11) and advanced hepatocellular carcinoma (12). However, the duration of effect is often short in clinical trials (13). In preclinical models a number of tumors do not respond at all, or respond initially but become resistant at a late stage of VEGF inhibition (14, 15). In some experimental cases, such therapy may even increase tumor invasiveness and metastasis (16, 17). A further problem is that although this therapy is highly specific, patients are not selected on the basis of pathways of sensitivity or resistance in their tumors. Thus, tumor resistance to VEGF inhibition has become a major obstacle to the effectiveness of antiangiogenic agents in the clinic (18, 19). Clearly, understanding the resistance mechanisms will enhance anti-VEGF efficacy by developing new therapeutic approaches or rational drug combinations.

Notch signaling is a conserved pathway affecting many biological processes including angiogenesis (20). Ligand

Authors' Affiliations: [1]Molecular Oncology Laboratories, Department of Oncology, Weatherall Institute of Molecular Medicine, John Radcliffe Hospital; [2]Department of Chemistry and Pharmacology, University of Oxford, Oxford, United Kingdom; [3]Preclinical Oncology/Antibody Discovery and Protein Engineering, Gaithersburg, Maryland; and [4]Histopathology laboratory, Cancer Research UK London Research Institute, London, United Kingdom

Note: Supplementary data for this article are available at Cancer Research Online (http://cancerres.aacrjournals.org/).

Corresponding Authors: Ji-Liang Li or Adrian L. Harris, Molecular Oncology Laboratories, Weatherall Institute of Molecular Medicine, University of Oxford, John Radcliffe Hospital, Oxford OX3 9DS, United Kingdom. Phone: 44-1865-222354; Fax: 44-1865-222431;
E-mail: ji-liang.li@imm.ox.ac.uk or aharris.lab@imm.ox.ac.uk

doi: 10.1158/0008-5472.CAN-11-1704

©2011 American Association for Cancer Research.

binding to the Notch receptor results in 2 successive proteolytic cleavages of the receptor. The second cleavage, catalyzed by γ-secretase, releases the Notch intracellular domain (NICD), which translocates to the nucleus where it activates the transcription of downstream targets such as EphrinB2, Hes1, and Hey1 (20). DLL4, the latest identified Notch ligand, is predominantly expressed in arterial endothelial cells (EC) during embryonic development, and haploinsufficiency of DLL4 leads to embryonic lethality from severe vascular defects (21). DLL4-Notch signaling inhibits physiologic angiogenesis by reducing the number of tip cells and thus decreasing angiogenic sprouting (22, 23). In adults, however, we have shown that DLL4 is strongly upregulated in tumor vasculature (24–28). Alterations of DLL4 expression inhibit multiple EC functions important in angiogenesis (28–30). Recently, we, and other groups, showed that DLL4-Notch signaling regulates tumor growth by decreasing angiogenesis but improving vascular function; conversely, blockade of DLL4-Notch signaling strikingly increases nonproductive angiogenesis but reduces tumor growth (26, 31–33).

The VEGF pathway interacts with DLL4-Notch signaling in the vasculature (20). VEGF induces the expression of DLL4 and Notch1 (28, 32, 34), while DLL4-Notch signaling reduces signaling in the VEGF pathway by decreasing VEGFR2 expression and increasing VEGFR1 expression (28–30, 32, 34). These characteristics have attracted many groups to further address the roles of DLL4 in tumor response to antiangiogenic therapy (26, 31, 32). Here, we report that DLL4-Notch signaling-mediated tumor resistance to anti-VEGF therapy by inducing the formation of larger vessels, which no longer depend on VEGF signaling, and by activating multiple other signaling pathways.

Materials and Methods

Cell culture

U87GM (U87, human glioblastoma) and HT1080 (human fibrosarcoma) cell lines were obtained from Cancer Research UK Cell Services. Generation of U87-EV and U87-DLL4 cells and growth conditions were described previously (26).

Xenograft mouse models

All protocols were carried out under Home Office regulations (26). The tumor cells (10^7 for U87, 5×10^6 for HT1080) were implanted into 6- to 8-week-old female BALB/c SCID mice (Harlan Sprague Dawley, Inc.) s.c. with 100 μL of cell suspension with an equal volume of Matrigel (BD Bioscience). Each group consisted of 5 mice. Tumor growth was monitored and measured using calipers. Tumor volume was calculated from a formula ($V = L \times W \times H \times \pi/6$). When used, dibenzazepine (DBZ) and bevacizumab were injected intraperitoneally (i.p.) every 3 days at a dose of 8.1 mmol/kg and 10 mg/kg, respectively. DBZ was resuspended in 0.5% (w/v) Methocel E4M and 0.1% (w/v) Tween 80. Anti-EphrinB2 and sEphB4 were given i.p. 3 times a week at a dose of 20 mg/kg, respectively. Sorafenib was dissolved in a 50% Cremophor EL/50% ethanol as a stock solution (4×); once the compound was in solution, the aqueous component was added gradually to generate the dosing solution (12.5% Cremophor EL/12.5% ethanol/75% water; ref. 5). Sorafenib was administered daily at 60 mg/kg via oral gavage. PD173074 was given daily at 60 mg/kg in 50 mmol/L sodium lactate buffer, pH4.0 by oral gavage. Each animal experiment was repeated at least for 2 to 3 times.

Immunohistochemistry

The mouse CD31 and NG2 (desmin or α-SMA) stainings on cryostat sections were done as previously described (26). Immunohistochemistry on paraffin sections at 4 μm was done after antigen retrieval in Tris-EDTA buffer, pH 9.0 or in citrate buffer, pH 6.0 (for FGF2) in a Decloaker (Biocare Medical). Primary antibodies used were against CA9 (M75, 1/75, 1 hour), VEGF (VG1, 5 μg/mL, at 4°C for 16 hours), VEGFR3 (AF743, 1/125, 35 minutes), and FGF2 (sc79, 1/500, 1 hour). Tumor vessels were detected on paraffin sections by rat anti-CD34 monoclonal antibody (MEC14.7, 1/250, 1 hour) using a Novolink kit (Leica Microsystems) after the antigen was retrieved in retrieval buffer (Dako R1669). Primary antibodies were washed off in PBS and detected using a polymer-based system (Dako). The peroxidase reaction was developed using diaminobenzidine provided in the kit. Slides were washed and mounted in aqueous mountant.

Quantitative real-time PCR

RNA extraction from xenograft tumors, quantitative real-time PCR (qPCR) protocol, *mHey1* and *β-actin* primers were previously described (26).

Western blotting

Protein extraction and Western blotting was done using standard techniques (28).

In situ hybridization

Mouse VEGFR2 mRNA was specifically localized in formalin-fixed tissue using an antisense riboprobe synthesized with SP6 RNA polymerase using ^{35}S-UTP (~800 Ci/mmol) and a plasmid encoding the 5′-end 2619bp of mouse VEGFR2. The riboprobe was used without hydrolysis (28).

Statistics

All data are presented as mean ± SEM. Statistical analysis including *t* test for 2 groups or 1-way ANOVA for multiple groups, and parametric generalized linear model with random effects for tumor growth were done using GraphPad Prism 4.0b software. Statistical significance is indicated by *, where $P < 0.05$, and **, where $P < 0.01$.

Results

DLL4-Notch signaling mediates tumor resistance to VEGF inhibition

SCID mice were implanted with U87GM cells that were transduced with empty vector retroviruses (U87-EV) or DLL4-encoded retroviruses (U87-DLL4) and treated with bevacizumab. DLL4 promoted tumor growth and reduced

mouse survival, whereas bevacizumab inhibited tumor growth and increased animal survival of both U87-EV and U87-DLL4 tumors when the treatment was started on the day of tumor implantation (Fig. 1A) (26). To mimic the clinical situation where antitumor therapies are initiated only after patient has an established or advanced tumor, we initiated anti-VEGF treatment when the tumor reached 150 mm^3 in size. Administration of bevacizumab was still effective in inhibiting the growth and improving animal survival of U87-EV tumors. In sharp contrast, U87-DLL4 tumors exhibited an intrinsic resistance to bevacizumab (Fig. 1B). Thus, DLL4 expression mediates tumor resistance to anti-VEGF therapy.

We utilized DBZ, a small molecule inhibitor of γ-secretase to block Notch signaling. DBZ strongly inhibited Notch signaling *in vitro*, as shown by reduced protein levels of the activated NICD and the Notch target Hes1 in ECs (Supplementary Fig. S1). Five injections of DBZ inhibited U87-DLL4 tumor growth and improved animal survival (Fig. 1C); continuous administration of DBZ completely abolished the tumor growth stimulated by DLL4. The effect of DBZ on Notch signaling *in vivo* was confirmed by assessing mHey1 expression by qPCR (Supplementary Fig. S2).

Next, we assessed the ability of DBZ to resensitize U87-DLL4 tumors to VEGF inhibition, initiating the therapy when the tumor reached 150 mm^3 in size (Fig. 1D). For U87-EV tumors, DBZ only slightly inhibited the growth whereas bevacizumab delayed the growth; however, combining DBZ with bevacizumab resulted in a more striking inhibition of the growth. For U87-DLL4 tumors, DBZ significantly delayed the growth, particularly so at later points, whereas treatment with bevacizumab did not affect the growth at all. However, when treatments were combined, DBZ not only abolished the tumor resistance to bevacizumab but also synergistically enhanced the inhibition of tumor growth and improved the animal survival with bevacizumab.

Similar experiments with DBZ and bevacizumab were also done in the human fibrosarcoma HT1080 tumor model where the tumor exhibited an intrinsic resistance to VEGF inhibition. Similar therapeutic effects were observed (Supplementary Fig. S3), suggesting that blockade of endogenous Notch signaling by DBZ can also sensitize a tumor with intrinsic *de novo* resistance to anti-VEGF therapy.

DLL4-induced large vessels but not pericyte coverage contribute to anti-VEGF resistance

We investigated tumor neovasculature by immunostaining for the EC marker CD31 (Fig. 2ABC). DLL4 significantly reduced the vessel number but increased the vascular lumen size (26). DBZ increased the number of vessels by 30% and 120% in U87-EV and U87-DLL4 tumors, respectively and reduced the vascular lumen size in U87-DLL4 tumors.

Bevacizumab greatly decreased the vessel number by 12-fold in U87-EV tumors, while only moderately by 2.5-fold in U87-DLL4 tumors. However, bevacizumab did not affect vascular lumen size at all in U87-DLL4 tumors. In contrast, the combination therapy not only reduced the vessel number in both tumors but also disrupted the large vessels in U87-DLL4 tumors. Thus, the results suggest that the large vessels triggered by DLL4-Notch signaling contribute to the tumor resistance.

We costained for CD31 and the pericyte marker NG2 (Supplementary Fig. S4). DLL4 decreased the pericyte coverage of tumor vessels (26); DBZ increased the pericyte coverage in both U87-EV and U87-DLL4 tumors. However, bevacizumab alone did not affect the level of pericyte coverage in either tumor compared with their relative controls. In the tumors cotreated with DBZ and bevacizumab, the levels of vessel coverage by pericytes were similar to those observed in the tumors treated with DBZ alone.

Reductions in hypoxia and VEGF contribute to anti-VEGF resistance

Hypoxia increases VEGF production in tumors and we hypothesized reduced hypoxia would decrease VEGF expression and hence reduce tumor dependency on VEGF. We assessed hypoxia levels before and following therapeutic treatments as indicted by response of the hypoxia inducible factor-1 target carbonic anhydrase IX (CA9; Fig. 3AB). Expression of CA9 was lower in U87-DLL4 tumors compared with the U87-EV control. DBZ treatment significantly increased tumor hypoxia, as shown by strong CA9 staining in both tumor types. Bevacizumab also induced hypoxia/CA9 expression in U87-EV tumors because of reduced vessel numbers; however, it did not significantly increase hypoxia in U87-DLL4 tumors.

Combined DBZ and bevacizumab treatment increased tumor hypoxia much more efficiently than DBZ alone in either tumor type. In addition, the combination therapy not only increased the number of cells expressing CA9 but also the intensity of CA9 staining (Fig. 3A). Consistent with hypoxia (Fig. 3B), similar results were obtained for tumor necrosis (Fig. 3C). Less hypoxia and less necrosis in DLL4 tumors could be attributed to the persistence of functional large vessels in bevacizumab-treated DLL4 tumors.

We costained tumor tissues with anti-CA9 and anti-VEGF antibodies. VEGF staining was observed on vessels along with weak cytoplasmic positivity in the tumor which seemed to increase in intensity around necrotic areas (Fig. 3A). Overall, the relative proportional expression of tumoral VEGF in each group (Fig. 3D) was similar to CA9 in each group (Fig. 3B). The level of VEGF in U87-DLL4 tumors was much lower than in U87-EV tumors. VEGF staining on vessels was clearly detected in U87-EV tumors as opposed to very faint staining in U87-DLL4 tumors. DBZ increased VEGF expression in both tumor types. In addition, DBZ increased VEGF staining on vessels in U87-DLL4 but not U87-EV tumors. Bevacizumab significantly increased VEGF expression only in U87-EV but not U87-DLL4 tumors. Combined DBZ with bevacizumab substantially increased VEGF expression in both tumors but decreased the VEGF staining on vessels although this effect was much clearer in U87-EV than in U87-DLL4 tumors (Fig. 3A–D). Bevacizumab treated U87-EV tumors showed vascular disruption, a neutrophilic vasculitis, and fibrinoid necrosis, an effect that was notably absent in U87-DLL4 tumors. Taken together, these results suggest that blockade of Notch signaling by DBZ induced

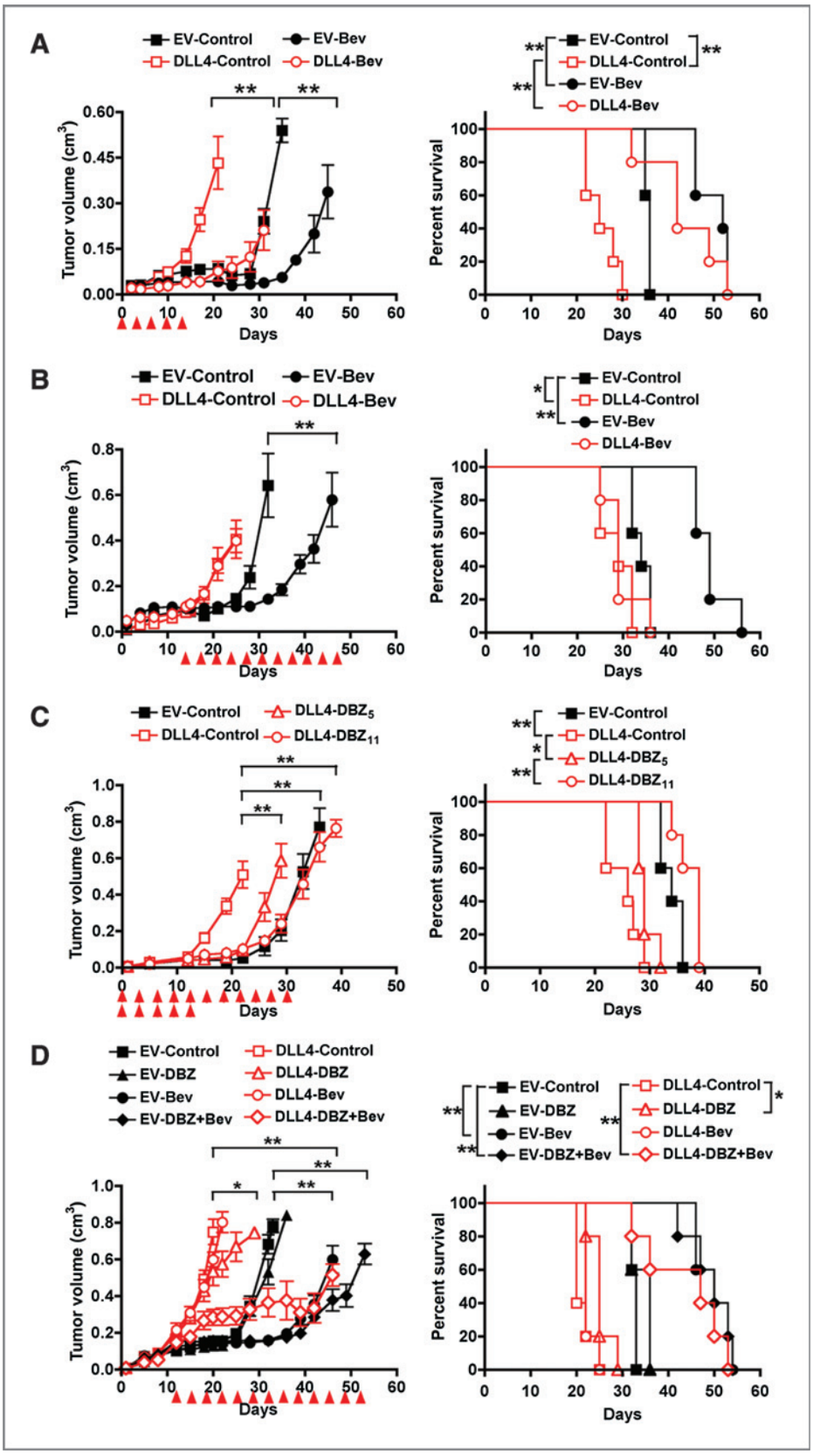

Figure 1. DLL4-Notch signaling-mediated tumor resistance to anti-VEGF therapy. A, tumor growth and animal survival of U87-EV and U87-DLL4 treated with bevacizumab (bev) or vehicle control, started on the same day of tumor implantation for 5 doses. B, tumor growth and animal survival of U87-EV and U87-DLL4 treated with bevacizumab or vehicle control, started from day 12 to the end of the experiment. C, DBZ reduced tumor growth and improved animal survival of U87-DLL4 *in vivo*, started on the same day of tumor implantation for 5 doses (DBZ_5) or 11 doses (DBZ_{11}). D, combination therapy by blockade of DLL4-Notch signaling with DBZ and inhibition of the VEGF pathway with bevacizumab reversed the tumor resistance to bevacizumab and synergistically inhibited tumor growth and increased animal survival. Treatment schedules are indicated by red arrowheads. Left panels show the tumor growth curves and right panels the animal survival curves. Mean ± SE, $n = 5$. *, $P < 0.05$, **, $P < 0.01$.

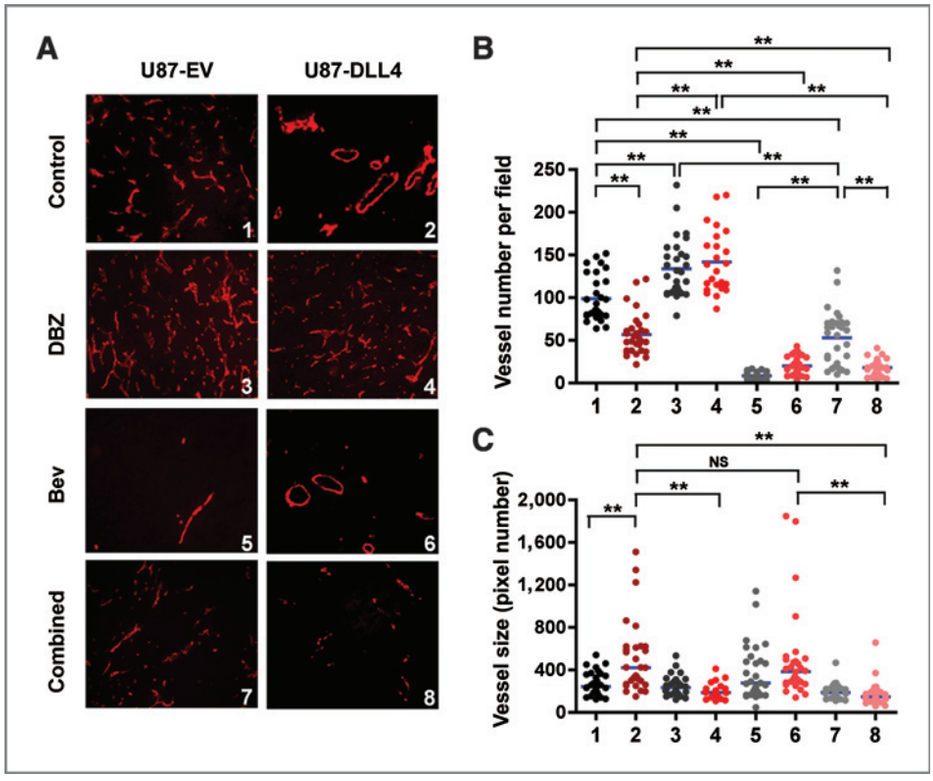

Figure 2. The large vessels induced by DLL4-Notch signaling contributed to the tumor resistance to anti-VEGF therapy. A, vascular morphology as revealed by mouse CD31 immunofluorescent staining (red) in frozen sections of tumor xenografts from Figure 1D. B quantification of the vessel number per field. C, quantification of the vessel size (pixels). DLL4 reduced vessel number but increased vessel size in tumors. DBZ increased vessel numbers of both U87-EV and U87-DLL4 tumors and abolished the large vessels. Bevacizumab reduced vessel numbers of both tumors but did not affect the vessel size of U87-DLL4 tumors. Combined therapy reduced vessel numbers of both tumors and abolished the large vessels. *, $P < 0.05$; **, $P < 0.01$. NS, no statistical difference. Each column represents: 1, U87-EV control; 2, U87-DLL4 control; 3, U87-EV DBZ; 4, U87-DLL4 DBZ; 5, U87-EV bevacizumab; 6, U87-DLL4 bevacizumab; 7, U87-EV combined DBZ with bevacizumab; 8, U87-DLL4 combined DBZ with bevacizumab.

tumor hypoxia and necrosis by disrupting the large vessels, and consequently increased the level of VEGF.

Alterations of expression of VEGFRs contribute to anti-VEGF resistance

We investigated the expression of VEGFR1 and VEGFR2 in stromal cells by qPCR using mouse specific primers. *In vitro*, DLL4 increased VEGFR1 (and soluble VEGFR1) expression and significantly decreased VEGFR2 expression in ECs (29, 30). *In vivo*, DLL4 increased the mRNA levels of VEGFR1 but VEGFR2 transcription was not deceased in U87-DLL4 tumors (Fig. 4A). We then analyzed VEGFR2 transcripts in tumor blood vessels using *in situ* hybridization (Fig. 4B). DLL4 reduced VEGFR2 expression only in the large vessels, whereas DBZ restored VEGFR2 expression in tumor vessels.

However, bevacizumab did not affect the expression of VEGFR2 in either U87-EV or U87-DLL4 tumors. In contrast, combined treatment of DBZ with bevacizumab restored the expression of VEGFR2 in the few remaining vessels, similar to the effects of DBZ alone. Indeed, the protein levels of VEGFR2 expressed in the large vessels were also decreased in U87-DLL4 tumors compared with U87-EV tumors (26). We further investigated the expression of VEGFR3. DLL4 reduced the mRNA level of VEGFR3 in human microvascular EC (hMEC-1) *in vitro* and the protein level in tumor neovasculature *in vivo* (Supplementary Fig. S5). Taken together, these results suggest that the large vessels were insensitive to VEGF due to the low expression of VEGFR2, and increased expression of VEGFR1 further diminished the sensitivity of VEGF-VEGFR2 signaling in tumors.

To inhibit mouse and human VEGF effects and exclude the possibility that antibody transport was a mechanism of resistance, we treated both tumor types with sorafenib to inhibit VEGFR1-R3. Sorafenib delayed the growth and improved animal survival of U87-EV tumors (Fig. 4C) but the efficiency was less than bevacizumab treatment (see Figure 1). Sorafenib marginally inhibited U87-DLL4 tumor growth and significantly improved animal survival of U87-DLL4 tumors, although this effect was greater than bevacizumab treatment alone (see Figure 1), presumably due to the blockade other RTKs (5).

Activation of FGF2-FGFR signaling contributes to anti-VEGF resistance

DLL4-Notch signaling significantly increased the expression of FGF2 in ECs *in vitro* (29) and in U87-DLL4 tumors *in vivo* at the protein level (Fig. 5A). We then treated both U87-EV and

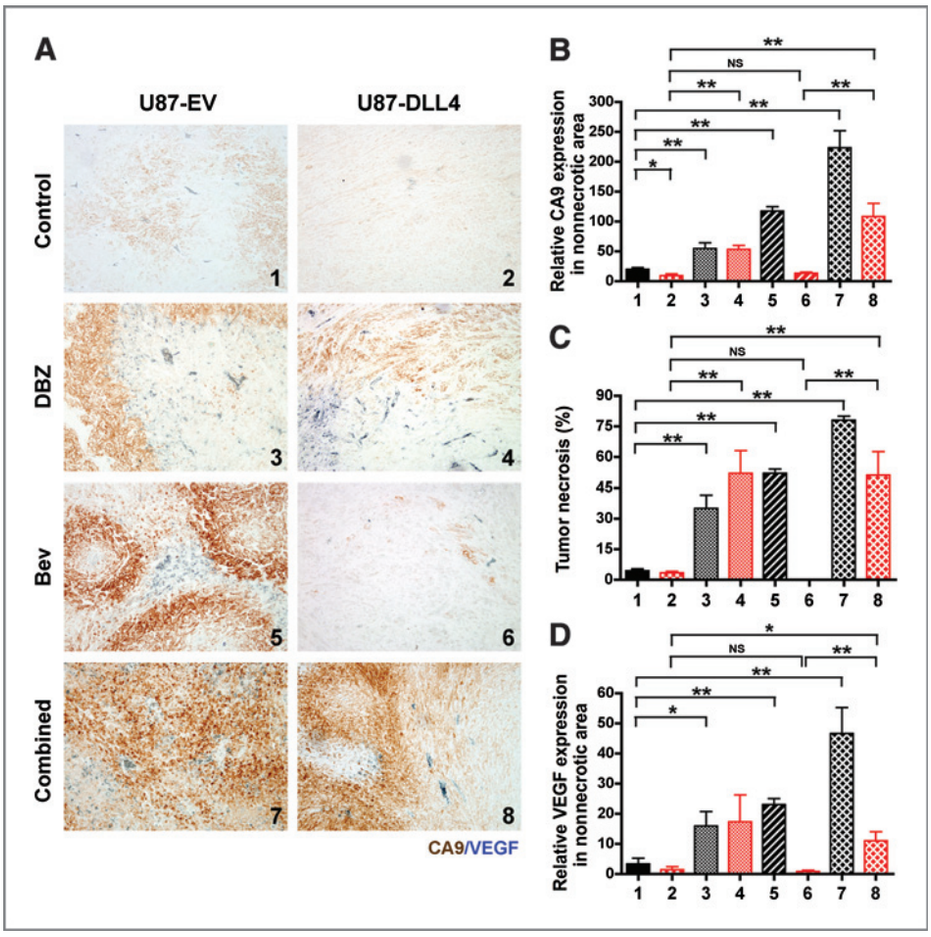

Figure 3. Reduction of hypoxia, necrosis and VEGF expression contributed to tumor resistance to anti-VEGF therapy. A, immunohistochemical staining for CA9 (brown) and VEGF (blue) in FFPE sections of tumor xenografts (from Figure 1D). B, quantification of CA9 staining in FFPE sections of tumor xenografts. C, quantification of tumor necrosis. D, quantification of VEGF staining in FFPE sections of tumor xenografts. DBZ alone increased hypoxia, VEGF expression and necrosis in both U87-EV and U87-DLL4 tumors. Bevacizumab alone effectively induced hypoxia, VEGF expression and necrosis in U87-EV tumors but not in U87-DLL4 tumors. However, combination DBZ with bevacizumab strongly increased hypoxia, VEGF expression and necrosis in both tumors. Mean ± SE, $n = 5$. *, $P < 0.05$; **, $P < 0.01$. NS, no statistical difference. Representative of each column was depicted in Figure 2.

U87-DLL4 tumors with PD173074 to inhibit FGF2-FGFR signaling (35). As little as 100 nmol/L of PD173074 could inhibit FGF2-FGFR signaling in ECs *in vitro*, reflected by elimination of tyrosine phosphorylation of ERK induced by FGF2 (Fig. 5B). In U87-EV tumors, PD173074 did not significantly inhibit the growth but slightly enhanced the efficacy of bevacizumab (Fig. 5C). In contrast, PD173074 slightly inhibited U87-DLL4 growth but significantly improved the tumor response to bevacizumab in the combination treatment (Fig. 5D).

Activation of EphB4-EphrinB2 signaling contributes to anti-VEGF resistance

The expression of EphB4 and EphrinB2 in tumors was assessed by qPCR. EphB4, but not EphrinB2, was significantly upregulated in U87-DLL4 tumors compared with the control (Fig. 6A), suggesting that EphB4-EphrinB2 signaling is enhanced as a result of increased EphB4 in the tumor. We therefore treated both tumor types with anti-EphrinB2 antibody or soluble EphB4 protein (sEphB4) that inhibit internalization and phosphorylation of EphrinB2, respectively. Single therapy with anti-EphrinB2 or sEphB4 did not significantly affect the growth of either tumor type (Fig. 6B), but combined anti-EphrinB2 or sEphB4 with bevacizumab significantly inhibited the growth and improved survival of U87-DLL4 tumors (Fig. 6C). Neither anti-EphrinB2 nor sEphB4 enhanced the efficacy of bevacizumab in combination treatments in U87-EV tumors (Supplementary Fig. S6). Thus, the results suggest that increased EphrinB2 reverse signaling in DLL4-tumors contributes to the tumor resistance to anti-VEGF therapy.

We investigated tumor neovasculature further by immunostaining for CD31 (Fig. 6D). Anti-EphrinB2 or sEphB4 significantly reduced the vessel number but not the vessel size in U87-EV tumors. However, both anti-EphrinB2 and sEphB4 increased the vessel number and reduced the vessel size in U87-DLL4 tumors. Combined anti-EphrinB2 or sEphB4 with bevacizumab not only decreased the vessel number but also abolished most, if not all, of the large vessels in DLL4 tumors. Taken together, the results suggest that blockade of EphrinB2 reverse signaling partially resensitized the tumor response to anti-VEGF therapy by disrupting the majority of large vessels induced by DLL4-Notch signaling.

Discussion

Multiple mechanisms are involved in tumor resistance to anti-VEGF therapy. These include preexistence/activation of alternative angiogenic pathways, recruiting vascular

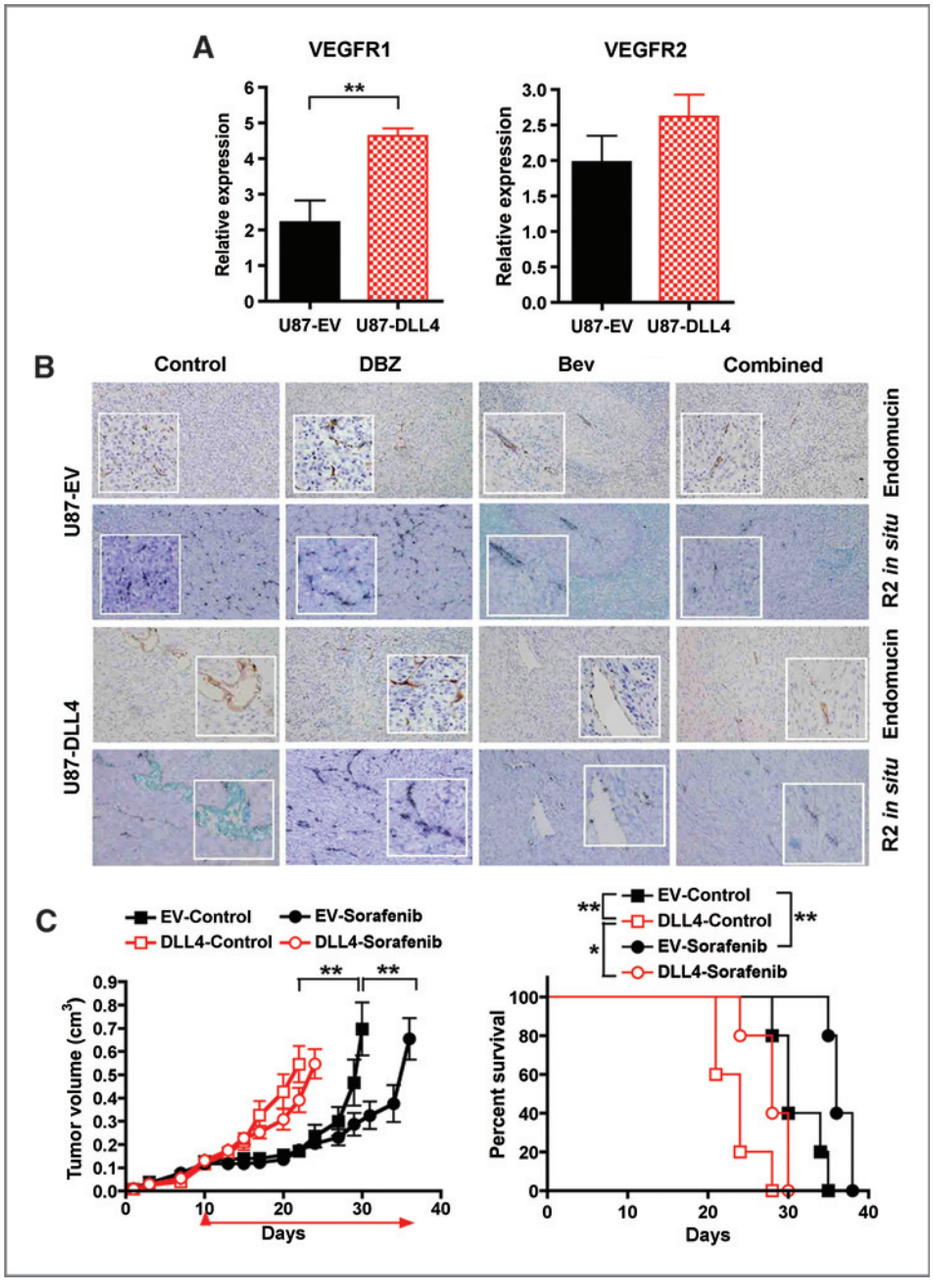

Figure 4. Alterations of VEGF receptors contributed to tumor resistance to anti-VEGF therapy. A, quantification of the *in vivo* expression of VEGF receptors by qPCR in U87-EV and U87-DLL4 tumors. VEGFR1, but not VEGFR2, was upregulated in DLL4 tumors. B, *in situ* hybridization for VEGFR2 in both tumors. Immunohistochemical staining for mouse endomucin showed tumor vessels. VEGFR2 mRNA was decreased in a proportion of the large vessels in U87-DLL4 tumors. C, sorafenib delayed tumor growth *in vivo*. Treatment with vehicle control or sorafenib by daily gavage was started from day 10 (indicated by a red arrow). Mean ± SE, $n = 5$. *, $P < 0.05$; **, $P < 0.01$.

progenitor cells from the bone marrow, increasing pericyte coverage, and enhanced capability of tumor cells to invade (13, 15). Here, we show that DLL4-Notch signaling mediates tumor resistance to bevacizumab *in vivo*. DLL4 is predominantly upregulated in tumor vasculature in preclinical models (21, 26, 31, 33) and in clinical tumor samples (24–28). However, DLL4 is also substantially upregulated in a subset of tumor cells in several human cancers including glioblastoma, colon, and breast cancer (24–28). Thus, our model by upregulating DLL4 in glioblastoma cells growing in immunodeficient mice is clinically relevant. Our findings may explain why so many patients in clinical trials do not respond to bevacizumab (13). Importantly, disruption of DLL4-Notch signaling by DBZ not only abolished the tumor resistance but also synergistically enhanced the therapeutic efficacy of bevacizumab.

All current clinical trials investigate the therapeutic efficiency of VEGF inhibitors without examining the expression of markers such as DLL4 and their subsequent impact in tumor and patient response to therapy. We investigated DLL4 expression in advanced breast tumors from AVF2119g, a randomized phase III trial by adding bevacizumab to capecitabine chemotherapy. When the tumors did not express DLL4 or had very low level expression, patients had a significant prolongation of progression free-survival upon

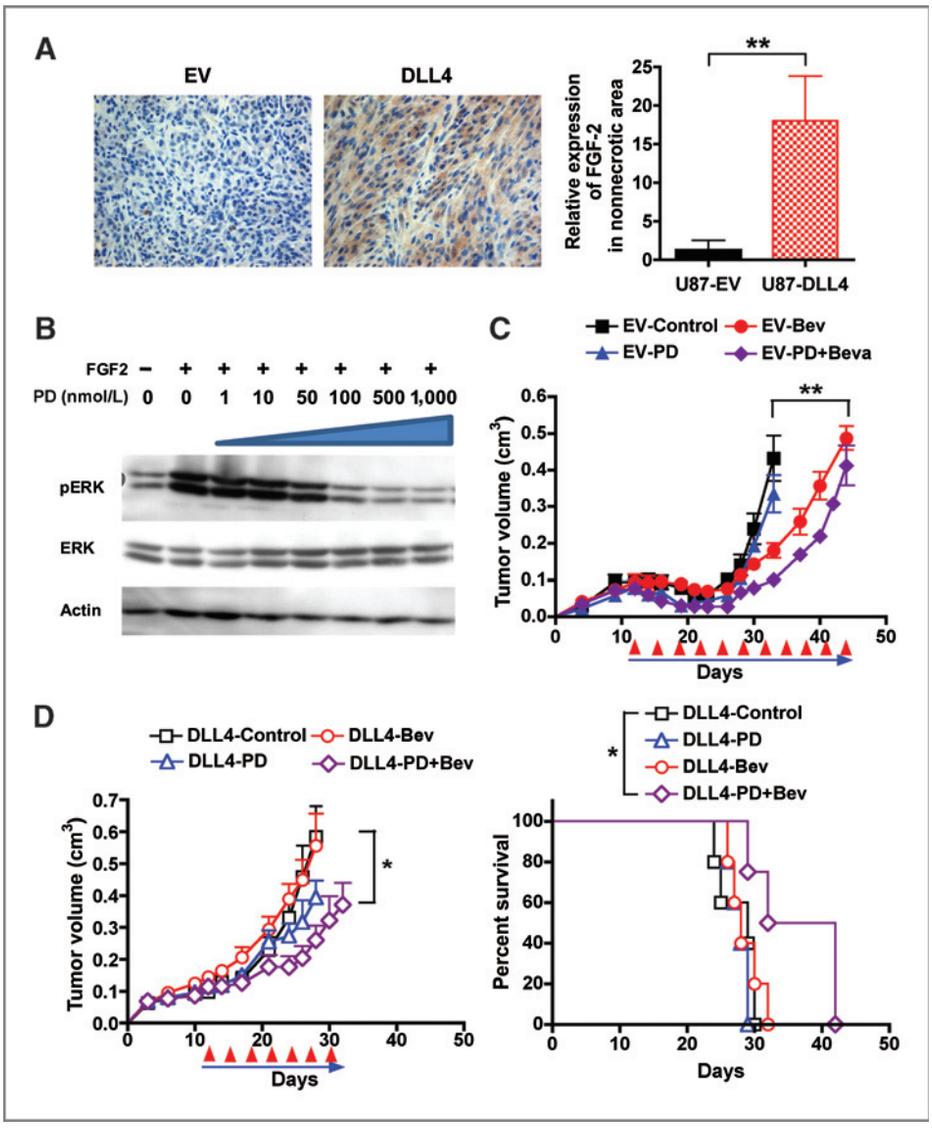

Figure 5. Upregulation of FGF2 by DLL4 contributed to tumor resistance to anti-VEGF therapy. A, immunochemical staining (right) and quantification (left) for FGF2 in xenograft tumors. B, the FGFR inhibitor, PD173074 (PD), inhibited the FGF2-induced phosphorylation of ERK (pERK) but did not affect the total ERK levels in HUVEC. C, PD173074 did not significantly affect tumor growth of U87-EV but had an additive effect with bevacizumab on the tumor growth. D, PD173074 marginally inhibited tumor growth of U87-DLL4 but significantly enhanced the therapeutic efficacy of bevacizumab in inhibition of tumor growth and increase of animal survival. Treatment schedules are indicated by red arrowheads for bevacizumab and a blue arrow for PD173074. Mean ± SE, $n = 5$. *, $P < 0.05$; **, $P < 0.01$.

adding bevacizumab; however, when DLL4 was highly expressed there was no benefit to the patients on adding bevacizumab (36). Thus our findings are clinically corroborated by the investigation of this randomized trial.

Our results indicated that the large vessels triggered by DLL4-Notch signaling play a central role in tumor resistance to bevacizumab. Bevacizumab only decreased the numbers of small vessels but did not affect the large vessels. These large vessels effectively delivered oxygen and nutrients to tumor cells as revealed by an increase in blood perfusion (26), resulting in a reduction in hypoxia and necrosis in DLL4 tumors. Reduced hypoxia decreased VEGF production and thus decreased the tumor dependency on VEGF. DLL4 decreased VEGFR2 expression in the large vessels and increased VEGFR1 expression in the tumor microenvironment, further diminishing the sensitivity of VEGF-VEGFR2 signaling. Blockade of DLL4-Notch signaling by DBZ abolished the large vessels, leading to a substantial increase of hypoxia and VEGF expression in DLL4 tumors, and consequently enhanced the therapeutic efficacy of bevacizumab. We found increased VEGF expression and although this may appear surprising in the context of bevacizumab treatment, we would still expect to detect intracellular VEGF in cells synthesizing or internalizing it. The observation of a neutrophilic vasculitis in the EV-tumors treated with bevacizumab, was most likely a response to the necrosis induced in the control tumors in contrast to the DLL4 tumors.

Increased and tight pericyte coverage of newly formed vessels has been shown to contribute to tumor resistance to anti-VEGF therapy (13, 37). However, we found that this is not the case in our models since DLL4 reduced the pericyte coverage and the reduction of pericyte coverage did not increase the sensitivity of bevacizumab. The SDF-1α/CXCR4 axis was reported to be essential for the pericyte recruitment in the PDGF-BB–expressing tumors (38). We previously reported that DLL4 inhibits CXCR4 expression *in vitro* and

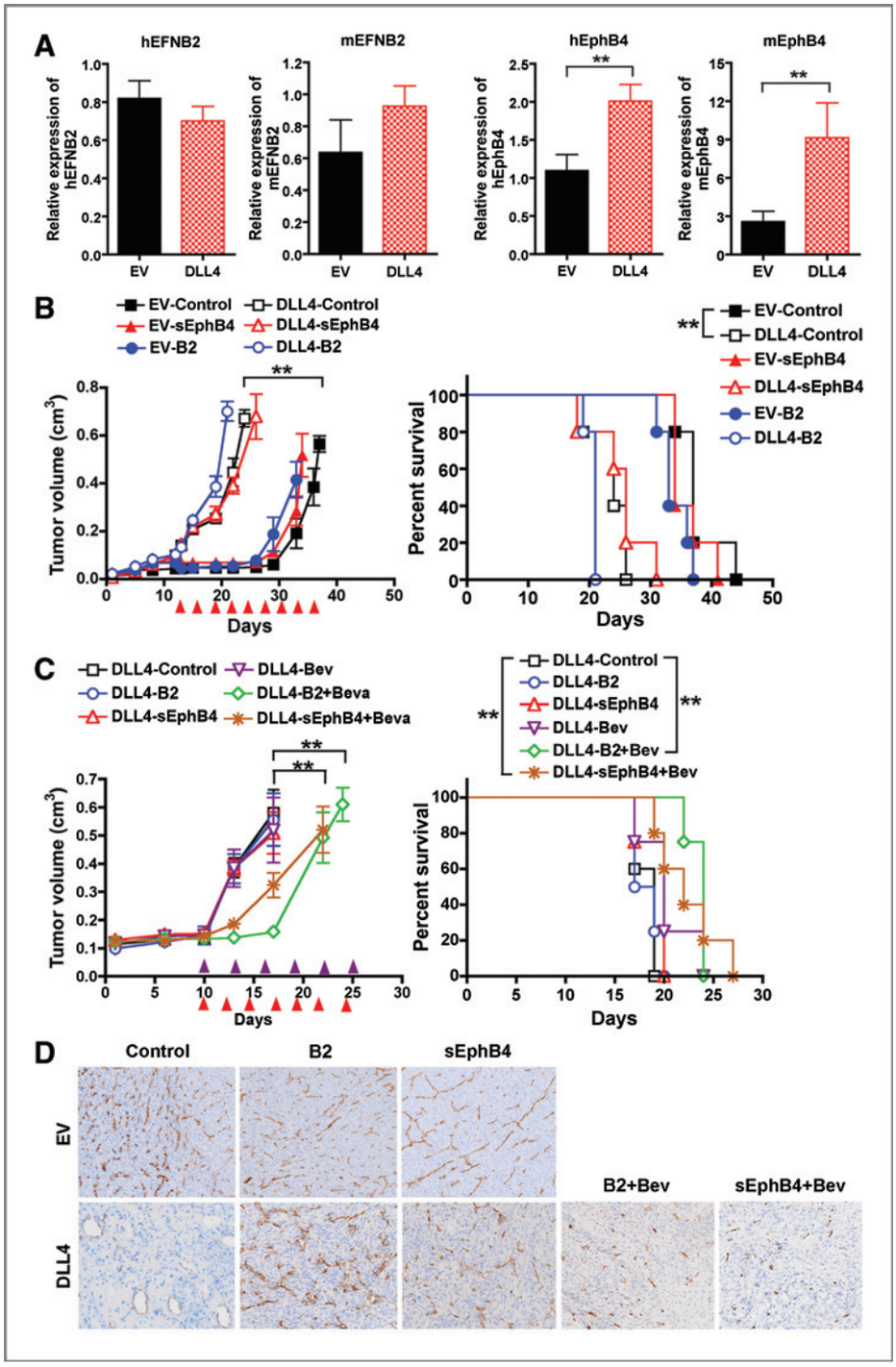

Figure 6. EphrinB2 reverse signaling contributed to the tumor resistance to anti-VEGF therapy. A, neither human nor mouse EphrinB2 was upregulated in U87-DLL4 tumors as revealed by qPCR. Both human and mouse EphB4 were increased in U87-DLL4 tumors as shown by qPCR. B, neither anti-EpherinB2 monoclonal antibody (B2) nor sEphB4 affected tumor growth (left) and animal survival (right) of both U87-EV and U87-DLL4 tumors. C, either anti-EphrinB2 antibody or sEphB4 sensitized the tumor response to bevacizumab (left) and improved animal survival (right) of U87-DLL4 tumors. D, anti-CD31 immunochemical staining showed that either anti-EphrinB2 antibody or sEphB4 decreased vessel numbers in U87-EV tumors but increased vessel numbers in U87-DLL4 tumors. Anti-EphrinB2 antibody or sEphB4 disrupted most of the large vessels. Combined anti-EphrinB2 or sEphB4 with bevacizumab not only decreased vessel numbers but also abolished the large vessels in U87-DLL4 tumors. Treatment schedules are indicated by red arrowheads (anti-EphrinB2 or sEphB4) and purple arrowheads (bevacizumab). Mean ± SE, $n = 5$. *, $P < 0.05$; **, $P < 0.01$.

in vivo (39), thus providing a mechanism for the decreased pericyte coverage in DLL4-tumors.

VEGFR3 is also important in tumor angiogenesis (40, 41) and is regulated by Notch signaling (23, 41, 42). In U87-DLL4 tumors, the protein level of VEGFR3 was significantly down-regulated, which may also produce resistance to VEGFR3 inhibitors. Sorafenib had a marginal effect on the growth of DLL4 tumors, suggesting that DLL4 may also contribute to tumor resistance to other antiangiogenic agents for example, blockers of VEGFR3 or VEGFC. FGF2 has been shown to confer tumor resistance to anti-VEGF signaling in the RIP-Tg2 pancreatic islet tumor model, some syngeneic mouse models, and *in vitro* cultures (14, 43, 44). We found that FGF2 was significantly increased and bevacizumab further

increased FGF2 expression in DLL4 tumors. However, the FGF2-FGFR inhibitor, PD173074, marginally inhibited the growth of DLL4 tumors but significantly improved the tumor response to bevacizumab, suggesting that FGF2-FGFR minimally contributes to the tumor resistance.

Recent studies showed that interaction of EphB4 with EphrinB2 inhibited EC sprouting and promoted circumferential growth of vessels, and reverse signaling via EphrinB2 decreased vessel numbers, but increased vessel lumen diameter, resulting in tumor progression (45, 46). EphrinB2 is a well-known downstream target of DLL4-Notch signaling (29, 30) and VEGF can effectively induce EphrinB2 but repress EphB4 (47). However, VEGF levels are reduced in DLL4 tumors due to reduced hypoxia, which may reverse this phenotype. Indeed, we found that EphB4, but not EphrinB2, was significantly higher in DLL4 tumors. sEphB4 was shown to antagonize forward and reverse signaling of EphrinB2, reduce vessel density and inhibit xenograft tumor growth (48). Anti-EphB4 antibody inhibited tumor angiogenesis and growth alone and in combination with bevacizumab (49). Combined therapy of sEphB4 with soluble DLL4 displayed cumulative efficacy against mouse insulinoma growth (50). We found that both sEphB4 and anti-EphrinB2 reduced the vessel number in U87-EV tumors, but increased the vessel number and reduced the vessel size in U87-DLL4 tumors. However, neither sEphB4 nor anti-EphrinB2 alone inhibited the growth of either tumor type. Importantly, both sEphB4 and anti-EphrinB2 resensitized the tumor response to bevacizumab by disrupting the large vessels, further highlighting the role of the large vessels in tumor resistance to anti-VEGF therapy. This also shows the heterogeneity of response to such therapies in different tumor models.

In conclusion, we found that DLL4-induced Notch signaling mediates tumor resistance to anti-VEGF therapy by inducing the formation of large vessels and activating multiple pathways in tumors. Importantly, blocking these bypass pathways had little effect on the more sensitive parent tumors, but showed greater effects in combination with bevacizumab in DLL4-tumors. The clinical implications for clinical trial design are that patients need to be carefully categorized by analysis of pathways in tumors, and combination strategies designed. Our findings provide a rational base for the development of novel strategies to overcome antiangiogenic resistance, and suggest that combination therapy by blocking both DLL4 and VEGF pathways may enhance the antitumor efficacy in the clinic, and DLL4 levels in tumor and vascular tissue should be assessed as a predictive biomarker.

Disclosure of Potential Conflict of Interest

No potential conflicts of interest were disclosed.

Acknowledgments

We thank Sandra Peak, Del Watling, Rachel Hayes, Sarah Scott, Christine White, and Barbara Cross (Cancer Research UK Biological Resources Unit) for assistance with xenograft experiments, Chunning Yang and Kristen Lekstrom (Antibody Discovery and Protein Engineering, MedImmune) for the production of anti-EphrinB2 antibody and sEphB4 recombinant protein, and Rosemary Jeffery (Cancer Research UK London Research Institute) for help with *in situ* hybridization.

Grant Support

This work was supported by Cancer Research UK and European Union 6th Framework Grant Angiotargeting.

The costs of publication of this article were defrayed in part by the payment of page charges. This article must therefore be hereby marked *advertisement* in accordance with 18 U.S.C. Section 1734 solely to indicate this fact.

Received May 20, 2011; revised July 17, 2011; accepted July 19, 2011; published OnlineFirst July 29, 2011.

References

1. Carmeliet P. Angiogenesis in life, disease and medicine. Nature 2005;438:932–6.
2. Gerber HP, Ferrara N. Pharmacology and pharmacodynamics of bevacizumab as monotherapy or in combination with cytotoxic therapy in preclinical studies. Cancer Res 2005;65:671–80.
3. Zhang D, Hedlund EM, Lim S, Chen F, Zhang Y, Sun B, et al. Antiangiogenic agents significantly improve survival in tumor-bearing mice by increasing tolerance to chemotherapy-induced toxicity. Proc Natl Acad Sci U S A 2011;108:4117–22.
4. Cao Y. Off-tumor target–beneficial site for antiangiogenic cancer therapy?Nat Rev Clin Oncol 2010;7:604–8.
5. Wilhelm SM, Carter C, Tang L, Wilkie D, McNabola A, Rong H, et al. BAY 43-9006 exhibits broad spectrum oral antitumor activity and targets the RAF/MEK/ERK pathway and receptor tyrosine kinases involved in tumor progression and angiogenesis. Cancer Res 2004;64:7099–109.
6. Hurwitz H, Fehrenbacher L, Novotny W, Cartwright T, Hainsworth J, Heim W, et al. Bevacizumab plus irinotecan, fluorouracil, and leucovorin for metastatic colorectal cancer. N Engl J Med 2004;350:2335–42.
7. Sandler A, Gray R, Perry MC, Brahmer J, Schiller JH, Dowlati A, et al. Paclitaxel-carboplatin alone or with bevacizumab for non-small-cell lung cancer. N Engl J Med 2006;355:2542–50.
8. Miller K, Wang M, Gralow J, Dickler M, Cobleigh M, Perez EA, et al. Paclitaxel plus bevacizumab versus paclitaxel alone for metastatic breast cancer. N Engl J Med 2007;357:2666–76.
9. Escudier B, Eisen T, Stadler WM, Szczylik C, Oudard S, Siebels M, et al. Sorafenib in advanced clear-cell renal-cell carcinoma. N Engl J Med 2007;356:125–34.
10. Escudier B, Pluzanska A, Koralewski P, Ravaud A, Bracarda S, Szczylik C, et al. Bevacizumab plus interferon alfa-2a for treatment of metastatic renal cell carcinoma: a randomised, double-blind phase III trial. Lancet 2007;370:2103–11.
11. Motzer RJ, Hutson TE, Tomczak P, Michaelson MD, Bukowski RM, Rixe O, et al. Sunitinib versus interferon alfa in metastatic renal-cell carcinoma. N Engl J Med 2007;356:115–24.
12. Llovet JM, Ricci S, Mazzaferro V, Hilgard P, Gane E, Blanc JF, et al. Sorafenib in advanced hepatocellular carcinoma. N Engl J Med 2008;359:378–90.
13. Bergers G, Hanahan D. Modes of resistance to anti-angiogenic therapy. Nat Rev Cancer 2008;8:592–603.
14. Casanovas O, Hicklin DJ, Bergers G, Hanahan D. Drug resistance by evasion of antiangiogenic targeting of VEGF signaling in late-stage pancreatic islet tumors. Cancer Cell 2005;8:299–309.
15. Shojaei F, Wu X, Malik AK, Zhong C, Baldwin ME, Schanz S, et al. Tumor refractoriness to anti-VEGF treatment is mediated by CD11b+Gr1+ myeloid cells. Nat Biotechnol 2007;25:911–20.
16. Ebos JM, Lee CR, Cruz-Munoz W, Bjarnason GA, Christensen JG, Kerbel RS. Accelerated metastasis after short-term treatment with a potent inhibitor of tumor angiogenesis. Cancer Cell 2009;15:232–9.

17. Paez-Ribes M, Allen E, Hudock J, Takeda T, Okuyama H, Vinals F, et al. Antiangiogenic therapy elicits malignant progression of tumors to increased local invasion and distant metastasis. Cancer Cell 2009;15:220–31.
18. Cao Y, Langer R. Optimizing the delivery of cancer drugs that block angiogenesis. Sci Transl Med 2010;2:15ps3.
19. Cao Y. Molecular mechanisms and therapeutic development of angiogenesis inhibitors. Adv Cancer Res 2008;100:113–31.
20. Li JL, Harris AL. Crosstalk of VEGF and Notch pathways in tumor angiogenesis: therapeutic implications. Front Biosci 2009;14: 3094–110.
21. Gale NW, Dominguez MG, Noguera I, Pan L, Hughes V, Valenzuela DM, et al. Haploinsufficiency of delta-like 4 ligand results in embryonic lethality due to major defects in arterial and vascular development. Proc Natl Acad Sci U S A 2004;101:15949–54.
22. Hellstrom M, Phng LK, Hofmann JJ, Wallgard E, Coultas L, Lindblom P, et al. Dll4 signaling through Notch1 regulates formation of tip cells during angiogenesis. Nature 2007;445:776–80.
23. Siekmann AF, Lawson ND. Notch signaling limits angiogenic cell behaviour in developing zebrafish arteries. Nature 2007;445:781–4.
24. Jubb AM, Soilleux EJ, Turley H, Steers G, Parker A, Low I, et al. Expression of vascular notch ligand delta-like 4 and inflammatory markers in breast cancer. Am J Pathol 2010;176:2019–28.
25. Jubb AM, Turley H, Moeller HC, Steers G, Han C, Li JL, et al. Expression of delta-like ligand 4 (Dll4) and markers of hypoxia in colon cancer. Br J Cancer 2009;101:1749–57.
26. Li JL, Sainson RC, Shi W, Leek R, Harrington LS, Preusser M, et al. Delta-like 4 Notch ligand regulates tumor angiogenesis, improves tumor vascular function, and promotes tumor growth *in vivo*. Cancer Res 2007;67:11244–53.
27. Patel NS, Dobbie MS, Rochester M, Steers G, Poulsom R, Le Monnier K, et al. Up-regulation of endothelial delta-like 4 expression correlates with vessel maturation in bladder cancer. Clin Cancer Res 2006;12: 4836–44.
28. Patel NS, Li JL, Generali D, Poulsom R, Cranston DW, Harris AL. Up-regulation of delta-like 4 ligand in human tumor vasculature and the role of basal expression in endothelial cell function. Cancer Res 2005;65:8690–7.
29. Harrington LS, Sainson RC, Williams CK, Taylor JM, Shi W, Li JL, et al. Regulation of multiple angiogenic pathways by Dll4 and Notch in human umbilical vein endothelial cells. Microvasc Res 2008;75:144–54.
30. Williams CK, Li JL, Murga M, Harris AL, Tosato G. Up-regulation of the Notch ligand Delta-like 4 inhibits VEGF-induced endothelial cell function. Blood 2006;107:931–9.
31. Noguera-Troise I, Daly C, Papadopoulos NJ, Coetzee S, Boland P, Gale NW, et al. Blockade of Dll4 inhibits tumor growth by promoting non-productive angiogenesis. Nature 2006;444:1032–7.
32. Ridgway J, Zhang G, Wu Y, Stawicki S, Liang WC, Chanthery Y, et al. Inhibition of Dll4 signaling inhibits tumor growth by deregulating angiogenesis. Nature 2006;444:1083–7.
33. Scehnet JS, Jiang W, Kumar SR, Krasnoperov V, Trindade A, Benedito R, et al. Inhibition of Dll4-mediated signaling induces proliferation of immature vessels and results in poor tissue perfusion. Blood 2007;109:4753–60.
34. Limbourg A, Ploom M, Elligsen D, Sorensen I, Ziegelhoeffer T, Gossler A, et al. Notch ligand Delta-like 1 is essential for postnatal arteriogenesis. Circ Res 2007;100:363–71.
35. Mohammadi M, Froum S, Hamby JM, Schroeder MC, Panek RL, Lu GH, et al. Crystal structure of an angiogenesis inhibitor bound to the FGF receptor tyrosine kinase domain. EMBO J 1998;17: 5896–904.
36. Jubb AM, Miller KD, Rugo HS, Harris AL, Chen D, Reimann JD, et al. Impact of exploratory biomarkers on the treatment effect of bevacizumab in metastatic breast cancer. Clin Cancer Res 2011;17: 372–81.
37. Willett CG, Boucher Y, di Tomaso E, Duda DG, Munn LL, Tong RT, et al. Direct evidence that the VEGF-specific antibody bevacizumab has antivascular effects in human rectal cancer. Nat Med 2004;10: 145–7.
38. Song N, Huang Y, Shi H, Yuan S, Ding Y, Song X, et al. Overexpression of platelet-derived growth factor-BB increases tumor pericyte content via stromal-derived factor-1alpha/CXCR4 axis. Cancer Res 2009;69: 6057–64.
39. Williams CK, Segarra M, Sierra Mde L, Sainson RC, Tosato G, Harris AL. Regulation of CXCR4 by the Notch ligand delta-like 4 in endothelial cells. Cancer Res 2008;68:1889–95.
40. Laakkonen P, Waltari M, Holopainen T, Takahashi T, Pytowski B, Steiner P, et al. Vascular endothelial growth factor receptor 3 is involved in tumor angiogenesis and growth. Cancer Res 2007;67: 593–9.
41. Tammela T, Zarkada G, Wallgard E, Murtomaki A, Suchting S, Wirzenius M, et al. Blocking VEGFR-3 suppresses angiogenic sprouting and vascular network formation. Nature 2008;454:656–60.
42. Shawber CJ, Funahashi Y, Francisco E, Vorontchikhina M, Kitamura Y, Stowell SA, et al. Notch alters VEGF responsiveness in human and murine endothelial cells by direct regulation of VEGFR-3 expression. J Clin Invest 2007;117:3369–82.
43. Fischer C, Jonckx B, Mazzone M, Zacchigna S, Loges S, Pattarini L, et al. Anti-PlGF inhibits growth of VEGF(R)-inhibitor-resistant tumors without affecting healthy vessels. Cell 2007;131:463–75.
44. Welti JC, Gourlaouen M, Powles T, Kudahetti SC, Wilson P, Berney DM, et al. Fibroblast growth factor 2 regulates endothelial cell sensitivity to sunitinib. Oncogene 2011;30:1183–93.
45. Erber R, Eichelsbacher U, Powajbo V, Korn T, Djonov V, Lin J, et al. EphB4 controls blood vascular morphogenesis during postnatal angiogenesis. EMBO J 2006;25:628–41.
46. Noren NK, Lu M, Freeman AL, Koolpe M, Pasquale EB. Interplay between EphB4 on tumor cells and vascular ephrin-B2 regulates tumor growth. Proc Natl Acad Sci U S A 2004;101:5583–8.
47. Scehnet JS, Ley EJ, Krasnoperov V, Liu R, Manchanda PK, Sjoberg E, et al. The role of Ephs, Ephrins, and growth factors in Kaposi sarcoma and implications of EphrinB2 blockade. Blood 2009;113: 254–63.
48. Kertesz N, Krasnoperov V, Reddy R, Leshanski L, Kumar SR, Zozulya S, et al. The soluble extracellular domain of EphB4 (sEphB4) antagonizes EphB4-EphrinB2 interaction, modulates angiogenesis, and inhibits tumor growth. Blood 2006;107:2330–8.
49. Krasnoperov V, Kumar SR, Ley E, Li X, Scehnet J, Liu R, et al. Novel EphB4 monoclonal antibodies modulate angiogenesis and inhibit tumor growth. Am J Pathol 2010;176:2029–38.
50. Djokovic D, Trindade A, Gigante J, Badenes M, Silva L, Liu R, et al. Combination of Dll4/Notch and Ephrin-B2/EphB4 targeted therapy is highly effective in disrupting tumor angiogenesis. BMC Cancer 2010;10:641.

Li et al., Figure S1

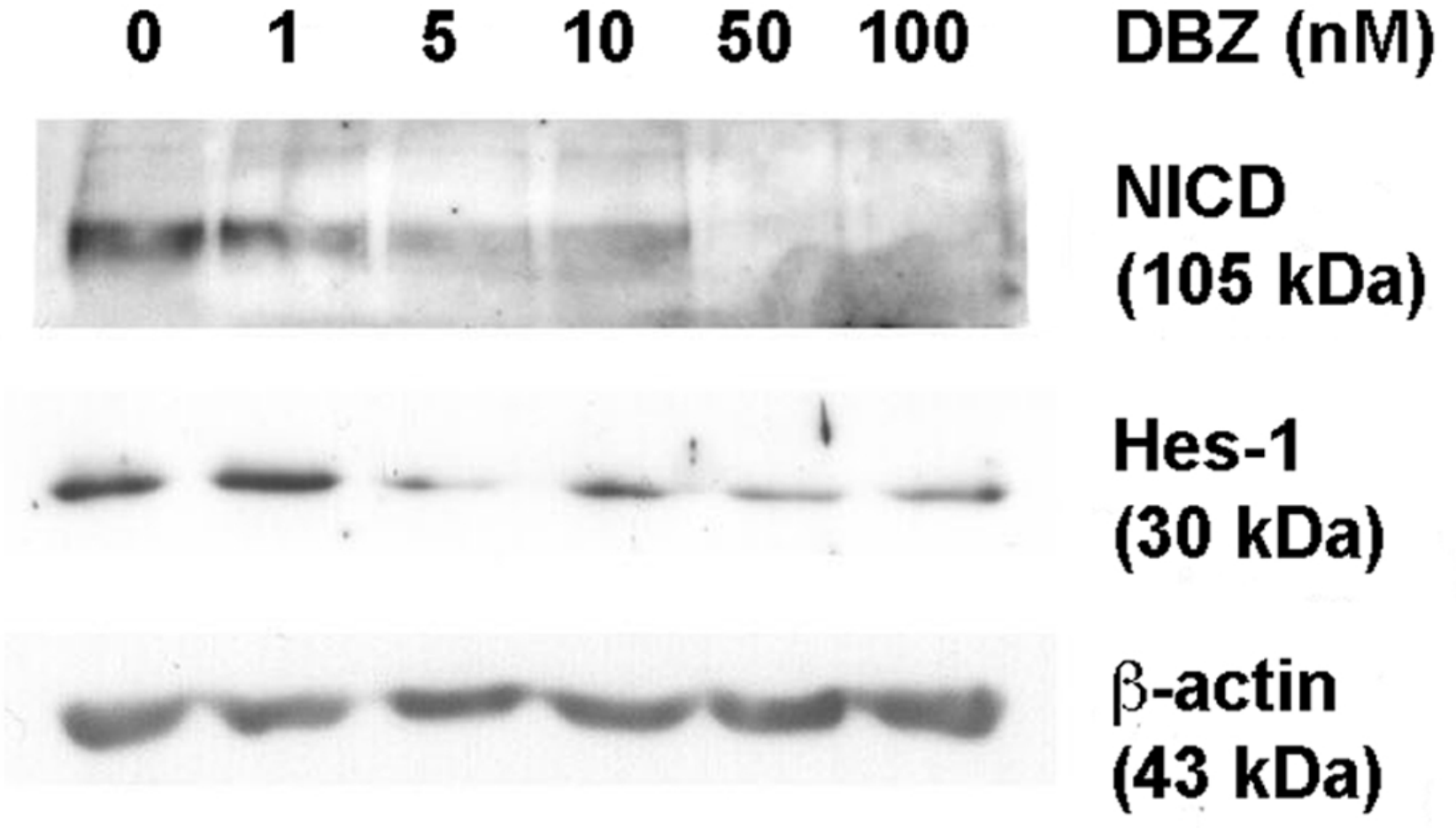

Li et al., Figure S2

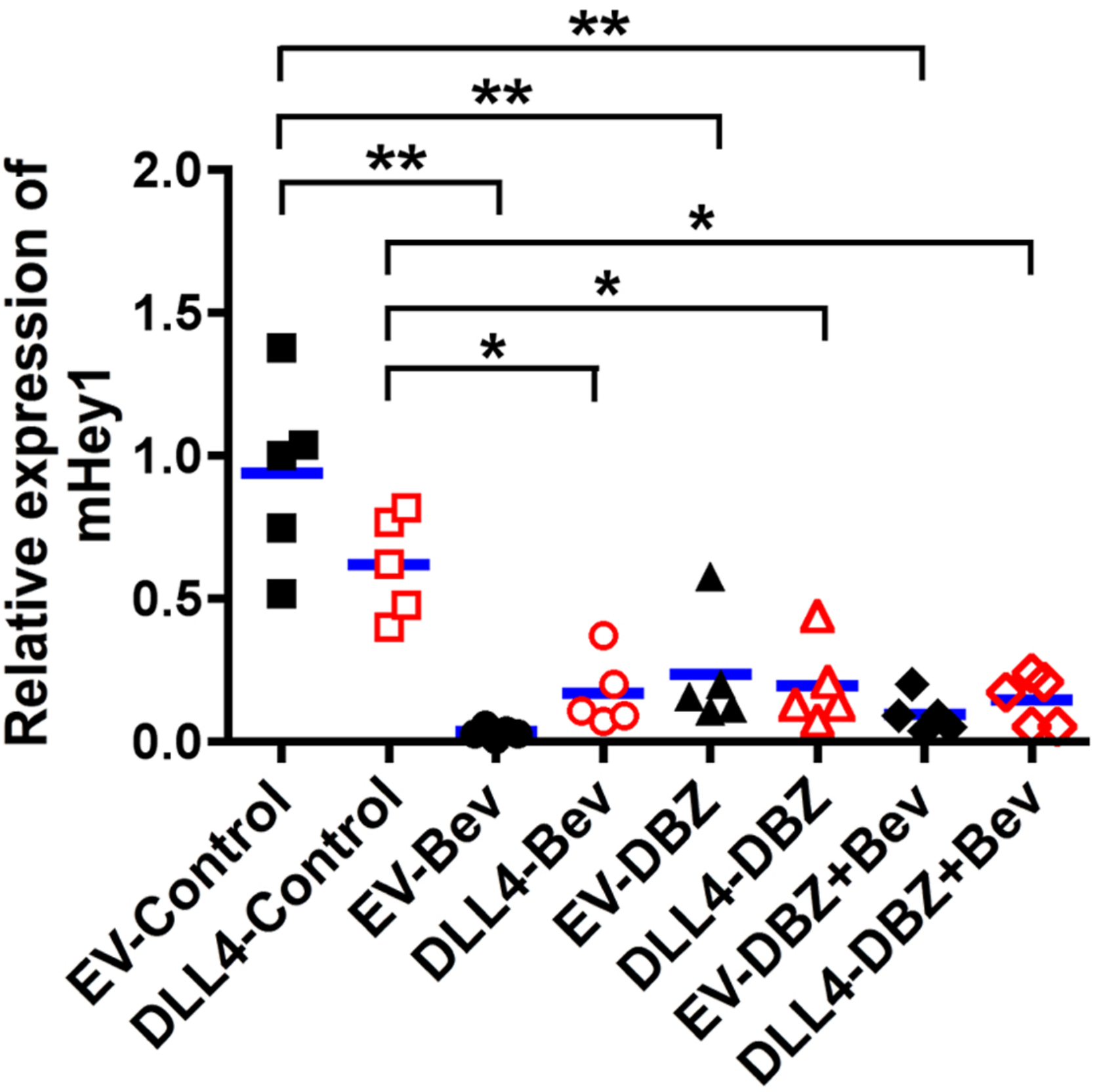

Li et al., Figure S3

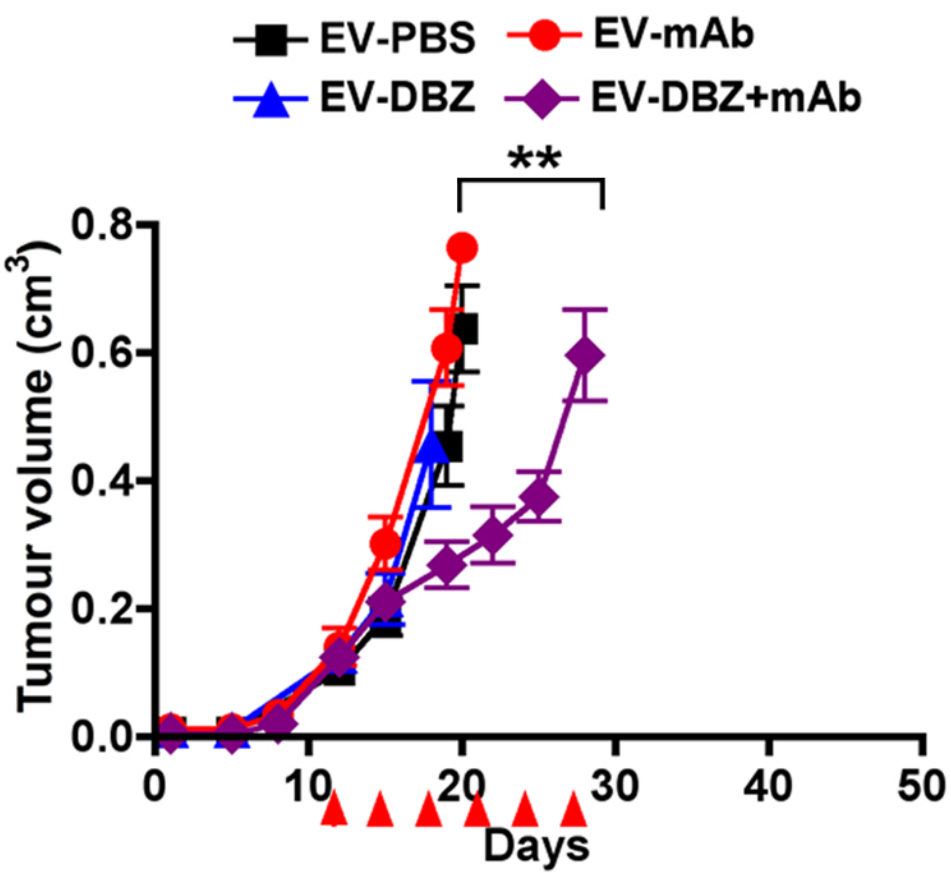

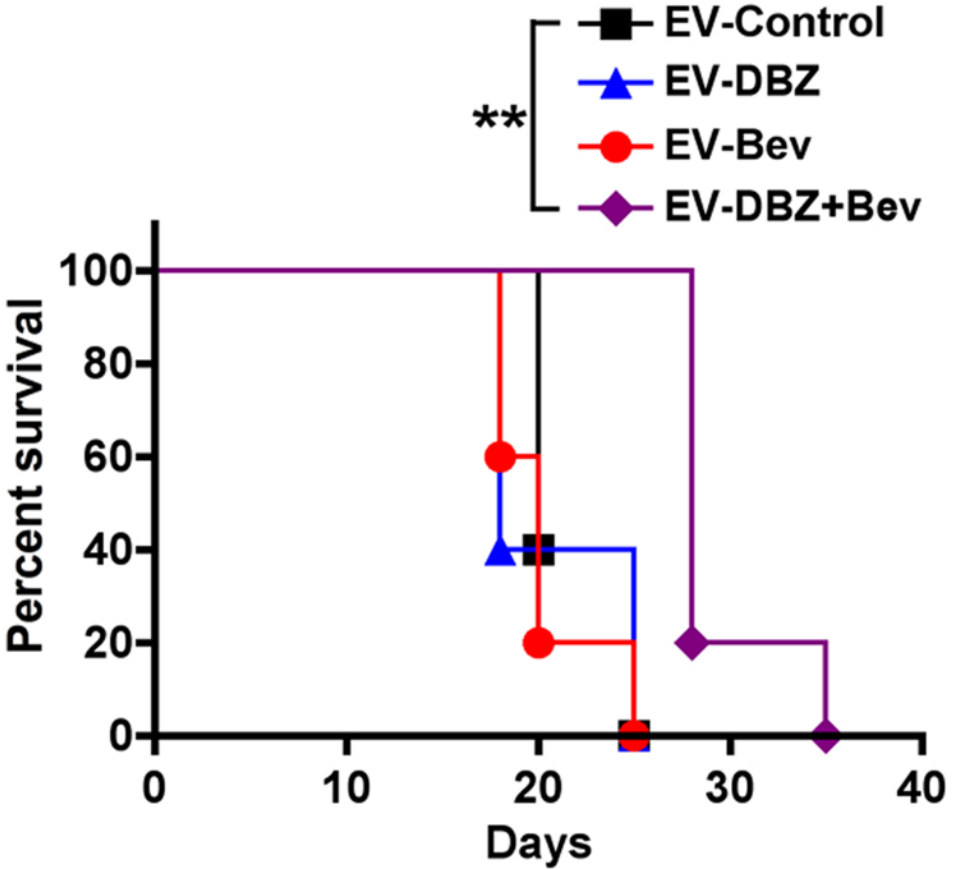

Li et al., Figure S4

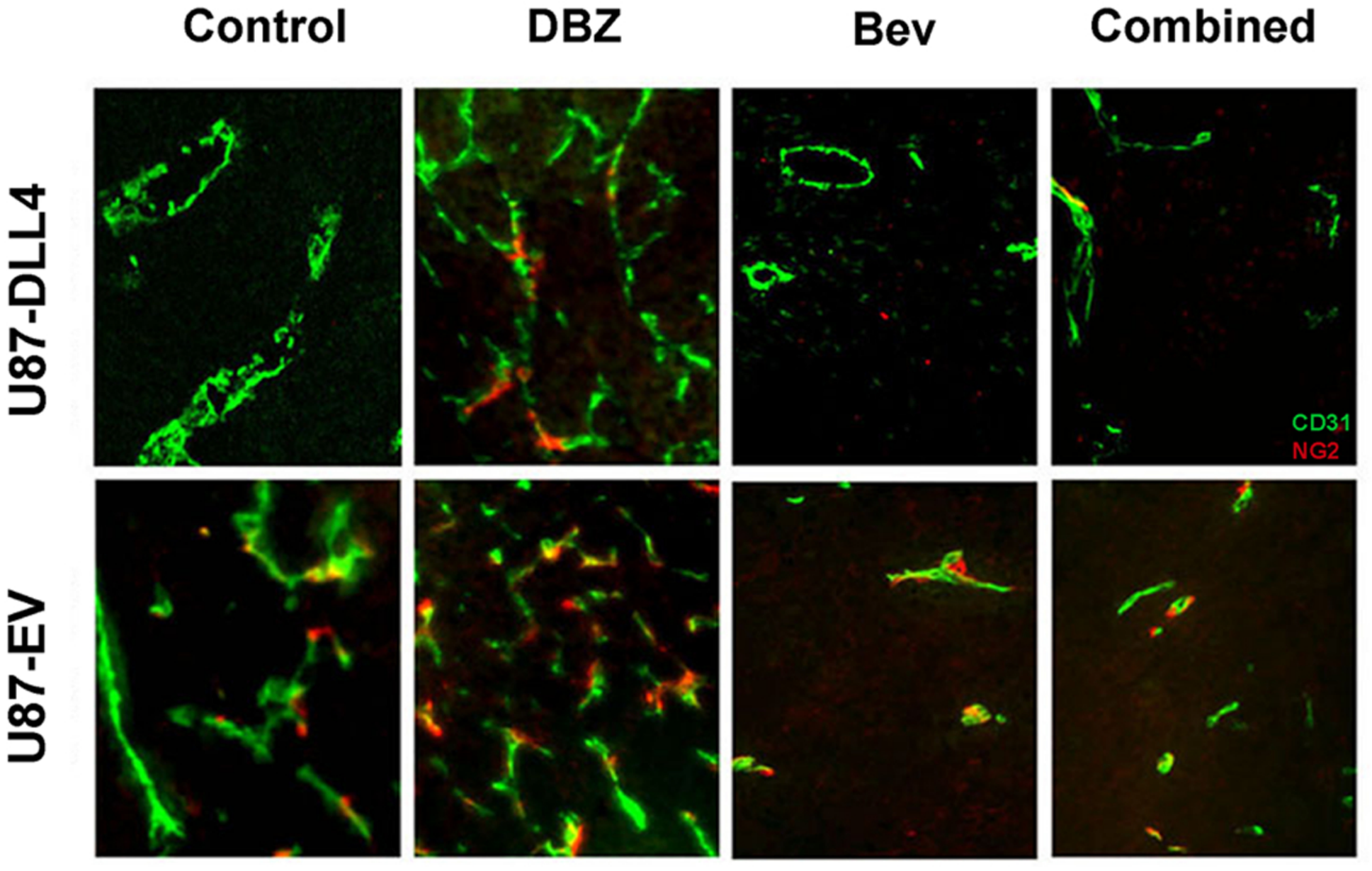

Li et al., Figure S5

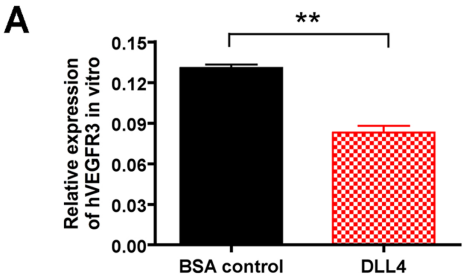

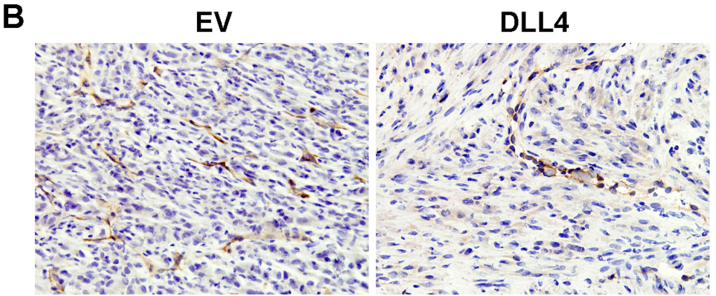

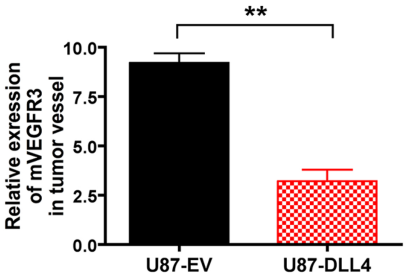

Li et al., Figure S6

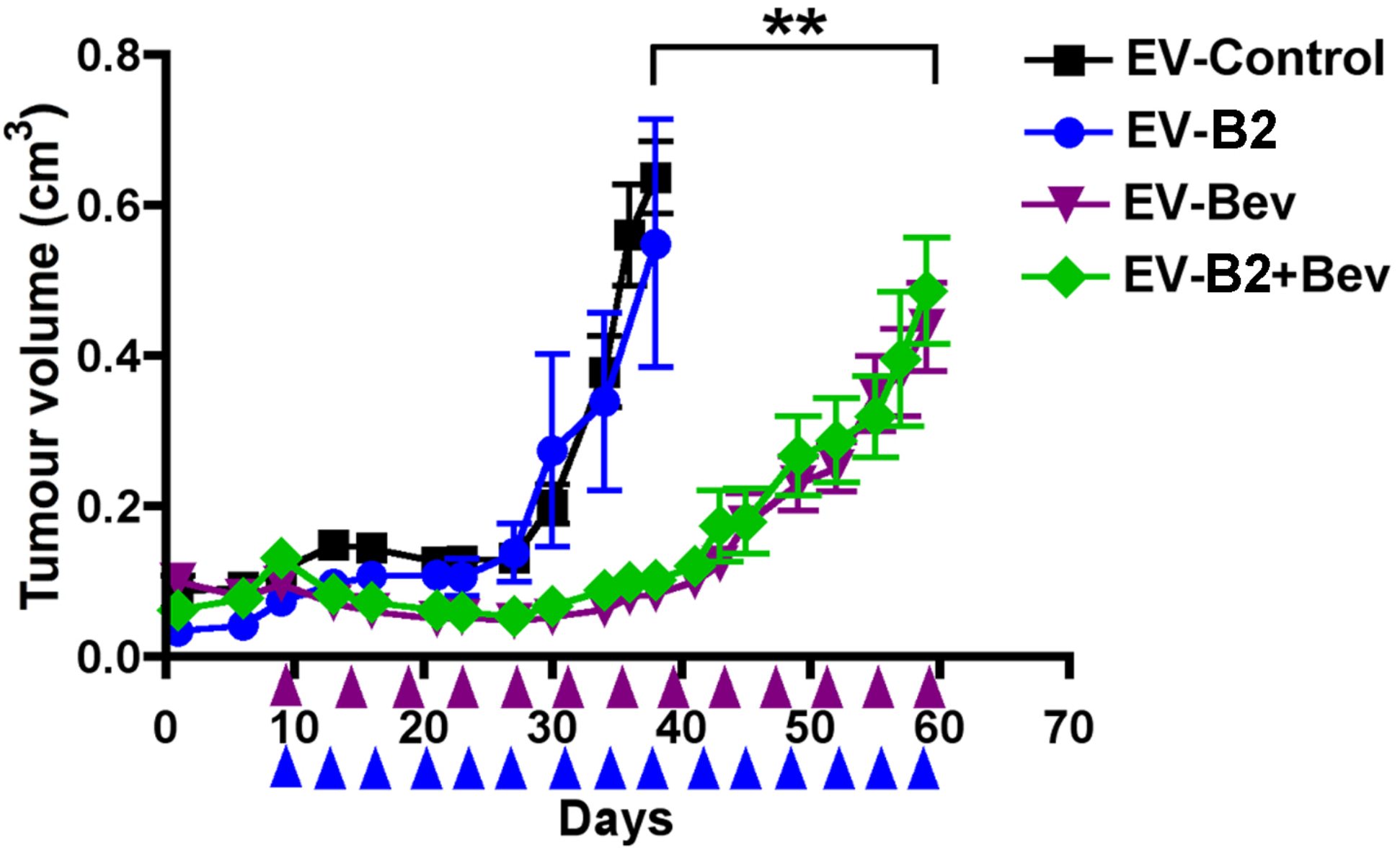

Supplementary Information

MATERIALS AND METHODS

Cell culture and reagents

U87GM (U87, human glioblastoma) and HT1080 (human fibrosarcoma) cell lines were obtained from Cancer Research UK Cell Services. Generation of U87-EV and U87-DLL4 cells and growth conditions were described previously (26). Mycoplasma contamination in cultured cells was excluded by using Lonza Mycoplasma Detection Kit. Dibenzazepine (DBZ) was purchased from Syncom (The Netherlands) at a purity of 99.8% at 232nm. PD173074 was purchased from TOCRIS Bioscience or made by C.P.M. and A.J.R.. Sorafenib (BAY54-9085) was generously provided by Bayer HealthCare Pharmaceuticals. Recombinant FGF2 was purchased from R&D Systems Europe Ltd. Antibodies were purchased from the following companies: Notch1IC, ERK, phosphorylated ERK (Cell Signalling) and β-actin (Sigma). Rabbit anti-FGF2 antibody (sc-79), recognizing both human and mouse FGF2, was purchased from Santa Cruz. The anti-Hes1 antibody was a gift from Tetsuo Sudo, Toray Industries, Japan. The anti-VEGF antibody (VG1, 1/1) that detects both human and mouse VEGF (isoform 121, 165, and 189) was obtained from Dako, and the M75 mouse monoclonal antibody against CA9 was purchased from Novus Biologicals (Littleton, CO). Monoclonal rat anti-mouse CD34 (clone MEC14.7) was obtained form AbD Serotec, UK. Anti-mouse, anti-rat, and anti-rabbit HRP conjugated secondary antibodies were from DAKO and anti-goat HRP was from Perbio. Human anti-EphrinB2 monoclonal antibody and recombinant sEphB4 protein (huEphB4 WT delta4R-HAS-His) were kindly supplied by MedImmune, USA. This anti-EphrinB2 antibody specifically recognized both human and mouse EphrinB2 and effectively neutralized the EphB4-EphrinB2 interaction. It binds to EphrinB2 on cell surface, preventing internalization and phosphorylation of EphrinB2, with an affinity of 5-10nM. The sEphB4 protein could compete for the EphB4-EphrinB2 interaction both in solid phase and cell based assays and thus agonized EphrinB2 as well as all its other binding partners.

Quantification of immunohistochemical staining

Necrosis was identified histologically on haematoxylin-eosin counterstained sections as areas displaying cells with basophilic pyknotic nuclei undergoing karyorrhexis and/or karyolysis, and scored as the percentage of the necrotic area in the entire full-face section. Immunohistochemical stainings of CA9, VEGF, VEGFR3 and FGF2 were scored for the intensity and percentage area of positive staining in viable tumor areas. The intensity was graded 1, 2 or 3 (corresponding to low, medium and high) and multiplied by the percentage area to produce an intensity percentage system score.

Primers for qPCR

RNA extraction from tumours, qPCR protocol, *mHey1* and *β-actin* primers were previously described (26). Other primers were listed as follows: mouse *VEGFR1* (*Flt1*, forward 5'-GGCCCGGGATATTTATAAGAAC-3' and reverse 5'-CCATCCATTTTAGGGGAAGTC-3'), mouse *VEGFR2* (*Kdr*, forward 5'-CAGTGGTACTGGCAGCTAGAAG-3' and reverse 5'-ACAAGCATACGGGCTTGTTT-3'), mouse *VEGFR3* (*Flt4*, forward 5'-GAATGAGAGCCCCGGAAC-3' and reverse 5'-GGTCTCCAGACCAGCAACTC-3'), mouse *Efnb2* (forward 5'-GATCCTCATGAAAGTTGGACAAG-3' and reverse 5'-AGCTCTGGACGTCTTGTTGG-3'), mouse *EphB4* (forward 5'-ACTGGGACATGAGCAACCA-3' and reverse 5'-TCTGCCAACAGTCCAGCAT-3'), human *EFNB2* (forward 5'-TGTAATTCCATCATCATCGTTGT-3' and reverse 5'-AAGTGTCGTAAGGCTCAATCG-3'), and human *EPHB4* (forward 5'-CGGATCCTACCCGAGTGA-3' and reverse 5'- TGTGTTCAGCAGGGTCTCTTC-3').

Western blotting

HUVECS isolated from fresh human umbilical cords were cultured in M199 media supplemented with 10% fetal calf serum and EC growth supplements. Tissue culture dishes (10cm), coated with 0.2% gelatin (w/v) in PBS, were pre-warmed to 37°C. After removed the coating solution, 10^6 HUVECs was added to each dish and incubated at 37°C in a CO_2 incubator for 48h such that cells were of sufficient confluency to allow endogenous Notch signalling. . Cells were treated with different concentrations of DBZ for 8h. Alternatively, cells were starved in M199 medium supplemented with 2% fetal calf serum for 24h and then pre-incubated with the PD173074 inhibitor at different concentrations for 1 hour before adding FGF-2 (15ng/ml) for 30min. Cells were lysed with urea lysis buffer. Protein extracts

(40μg) were separated by SDS-PAGE and Western blotting was performed using standard techniques (28).